An Enhanced Equivalent Circuit Model with Real-Time Parameter Identification for Battery State-of-Charge Estimation

Naseri, Farshid; Schaltz, Erik; Stroe, Daniel-Ioan; Gismero, Alejandro; Farjah, Ebrahim

Published in:
I E E E Transactions on Industrial Electronics

DOI (link to publication from Publisher):
10.1109/TIE.2021.3071679

Publication date:
2022

Document Version
Accepted author manuscript, peer reviewed version

An Enhanced Equivalent Circuit Model with Real-Time Parameter Identification for Battery State-of-Charge Estimation

Farshid Naseri, *Member, IEEE*, Erik Schaltz, *Member, IEEE*, Daniel-Ioan Stroe, *Member, IEEE*, Alejandro Gismero, Ebrahim Farjah, *Member, IEEE*

***Abstract*—This paper introduces an efficient modeling approach based on Wiener structure to reinforce the capacity of the classical Equivalent Circuit Models (ECMs) in capturing the nonlinearities of Lithium-ion (Li-ion) batteries. The proposed block-oriented modeling architecture is composed of a simple linear ECM followed by a static output nonlinearity block, which helps achieving a superior nonlinear mapping property while maintaining the real-time efficiency. The observability of the established battery model is analytically proven. This paper also introduces an efficient parameter estimator based on extended-kernel iterative recursive least squares algorithm for real-time estimation of the parameters of the proposed Wiener model. The proposed approach is applied for state-of-charge (SoC) estimation of 3.4 Ah 3.6 V NMC-based Li-ion cells using the extended Kalman filter (EKF). The results show about 1.5% improvement in SoC estimation accuracy compared with the EKF algorithm based on second-order ECM. A series of real-time tests are also carried out to demonstrate the computational efficiency of the proposed method.**

***Index Terms*—Equivalent Circuit Model (ECM), Extended Kalman Filter (EKF), Least Squares, Lithium-ion (Li-ion) Battery, State-of-Charge (SoC), Wiener Model.**

I. Introduction

With the advancement of Lithium-ion (Li-ion) battery technology, significant efforts have been placed on developing efficient battery models to fulfill specific objectives in Battery Management Systems (BMSs), e.g. State-of-Charge (SoC) and State-of-Health (SoH) estimation [1]. Many commercial vehicular BMSs employ low-cost microcontrollers with limited processing resources [2]. Thus, the battery model should be selected as a trade-off between the model accuracy and its real-time efficiency [2].

The literature regarding Li-ion battery modeling and state estimation is quite rich including several good review works that have been recently published on these topics [3], [4]. The battery models can be broadly categorized into three groups including: 1-Electrochemical models, 2- data-driven models, and 3-Equivalent Circuit Models (ECMs) [3]. The electrochemical models have a strong potential in capturing the kinetic and charge transfer dynamics [5], [6]. However, due to their computational complexity, the electrochemical models are not well-suited for online applications [3]. Data-driven models rely on extensive testing to collect large battery datasets and apply algorithms that can learn from the data in order to represent the behavior of battery in different operating regimes [7], [8]. The main challenge of the data-driven models is related to the time-consuming and costly training process [3]. The ECMs utilize electrical circuit components to represent the battery behavior in a comparatively simple and computationally efficient way [9], [10]. In [1], the partial least squares regression with the moving-window structure has been applied to the second-order ECM to obtain a series of piecewise linear battery models. The SoC estimation has been thus simplified by this approach because linear Kalman filter (KF) can be used for the developed linear model. In [9], a switched model based on the linear ECM has been proposed and used with the H_∞ observer to estimate the SoC. To predict the battery behavior, a second-order ECM has also been developed in [10], where a reduced states dimension is then established to estimate the SoC using the extended KF (EKF) algorithm. In [11], a temperature-dependent ECM has been developed and incorporated with the set membership technique for SoC estimation. The main feature of this method is that it handles the effects of the measurement noises on the estimation process. The second-order ECM has also been used in [12], where the adaptive EKF (AEKF) with forgetting factor strategy has been applied to estimate the SoC considering the temperature compensation. In [13], the first-order ECM has been established and used with the adaptive H_∞ filter algorithm for the SoC estimation. Despite using the first-order ECM, this method achieves a good performance due to the ability of the H_∞ filter in dealing with modeling uncertainties. Various algorithms have also been proposed for real-time estimation of the parameters of the ECMs including the Least-Squares (LS) algorithm and its variations such as Recursive LS (RLS) and weighted RLS filters [14]–[16], dual EKF (DEKF) [17], dual sigma-point KF (unscented KF) [18], particle filter [19], etc. Despite simplicity of the ECMs, it has been shown that these models sometimes fail to accurately capture some dynamics such as solid phase diffusion caused by large discharge currents [20] or dynamics at the over-potential regime [21]. To enhance the modeling capability, an autoregressive exogenous (ARX) model has been proposed in [22], where the numerical subspace state space

F. Naseri and E. Farjah are with the School of Electrical and Computer Engineering, Shiraz University, Shiraz, 71348-51154, Iran (email: f.naseri@shirazu.ac.ir, farjah@shirazu.ac.ir).

E. Schaltz, D. Stroe, and A. Gismero are with the Department of Energy Technology, Aalborg University, Aalborg, 9220, Denmark (email: esc@et.aau.dk, dis@et.aau.dk, aga@et.aau.dk).

This article has been accepted for publication in a future issue of this journal, but has not been fully edited. Content may change prior to final publication. Citation information: DOI 10.1109/TIE.2021.3071679, IEEE Transactions on Industrial Electronics

identification technique is applied for parameter estimation. Likewise, a hybrid modeling approach by combining the second-order ECM with an analytical model to improve the energy prediction performance has been proposed in [23]. Despite achieving a good nonlinear mapping property, these methods have limitation in terms of real-time efficiency, which challenges their application to large battery packs. Moreover, the real-time parameter estimation is not discussed in [23].

The high number of research works published recently shows that this subject is still an open problem. On one hand, higher-order battery models are needed to achieve proper transient and steady-state performances in predicting the battery voltage. On the other hand, the enhanced models increase complexity and necessitate more powerful and costly processors. Therefore, there is still a certain need to devise efficient models that suitably handle the battery nonlinearity at a reasonable computational cost. To this end, the novel trade-off considered in this paper is to reinforce the well-established battery ECMs through the so-called Wiener configuration. The proposed structure enhances the nonlinear mapping capacity of the linear ECMs while it is also easier to implement than the heavy-duty models [24]. Nevertheless, online identification of the Wiener model is challenging due to the unavailability of the intermediate signal between the linear and nonlinear segments [24]. To resolve this problem, in [25], the Wiener model is reformatted to multi-input single-output form and the model parameters are estimated using the classical RLS algorithm. However, this method involves regression equations that contain first and second derivatives of the battery measurements. Thus, the measurement noises might be strengthened. In this paper, an efficient method based on Extended-Kernel Iterative Recursive Least-Squares (EKIRLS) Algorithm is proposed to simultaneously estimate the parameters of the linear and nonlinear segments.

The contributions of this paper can be summarized as follows: (i) A Wiener model is established to enhance the nonlinear mapping potential of the ECMs. The proposed model has a strong capability in capturing battery dynamics and/or nonlinear voltage responses while it still offers relatively low computational complexity. (ii) An efficient online estimation mechanism based on the EKIRLS algorithm is proposed to estimate the parameters of the proposed model in real-time. (iii) The Wiener model is transformed to the state-space form, its observability is analytically proven, and finally, the model is used with the EKF algorithm for SoC estimation of the studied Nickel Manganese Cobalt (NMC)-based Li-ion battery cells.

The rest of this paper is organized as follows: The principles of the proposed approach are described in Section II. In Section III, the state-space representation and the EKF formulation are derived. The experimental results are presented and discussed in Section IV, where the Processor-in-the-Loop (PiL) test results are also presented to confirm the real-time efficiency. The proposed method is also compared with some other techniques and the results are provided in Section V. Finally, in Section VI, the main conclusions are provided.

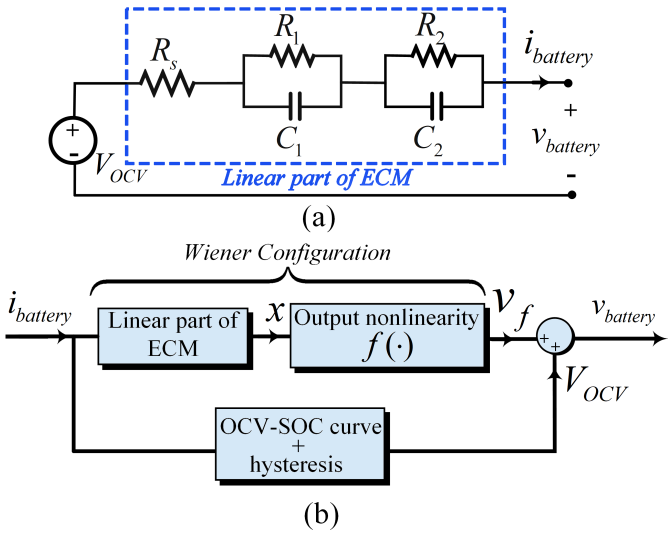

Fig. 1. (a) Structure of the second-order ECM (b) The proposed Li-ion battery model based on Wiener configuration

II. Modeling and Parameter Estimation Methods

The block diagram of the proposed model is shown in Fig. 1, where $i_{battery}$ (model input) and $v_{battery}$ (model output) are, respectively, the terminal current and voltage of the battery and x denotes the intermediate signal. The proposed Wiener model is composed of the linear part of the second-order ECM shown in Fig. 1(a) and an output nonlinearity term. In Fig. 1, V_{OCV} is the open-circuit voltage, R_s is the series resistance, and R_j and C_j are the resistance and capacitance of the jth RC network, respectively. The unique advantage of the proposed Wiener model is that it decomposes the nonlinear input-output relationship into two different interconnected segments and each segment separately represents the linear and nonlinear dynamics of the battery, which facilitates the parameter estimation process. The linear part of the model is represented using the Output-Error (OE) model as follows:

$$x(k) = \frac{B(z^{-1})}{A(z^{-1})} i_{battery}(k) \tag{1}$$

where z^{-1} is the unit back-shift operator, k is the sample index, and $A(z^{-1})$ and $B(z^{-1})$ are, respectively, z-polynomials with degrees n and m as follows:

$$A(z^{-1}) = 1 + a_1 z^{-1} + a_2 z^{-2} + ... + a_n z^{-n}$$

$$B(z^{-1}) = b_0 + b_1 z^{-1} + b_2 z^{-2} + ... + b_m z^{-m}$$

The battery terminal voltage $v_{battery}$ can be written as follows:

$$v_{battery} = f(x(k)) + V_{OCV} = f(\frac{B(z^{-1})}{A(z^{-1})} i_{battery}) + V_{OCV} \tag{2}$$

where $f(\cdot)$ is the output nonlinear function in the Wiener configuration. The system identification studies for obtaining $f(\cdot)$ and principles of the proposed EKIRLS algorithm are discussed in the following subsections.

This article has been accepted for publication in a future issue of this journal, but has not been fully edited. Content may change prior to final publication. Citation information: DOI 10.1109/TIE.2021.3071679, IEEE Transactions on Industrial Electronics

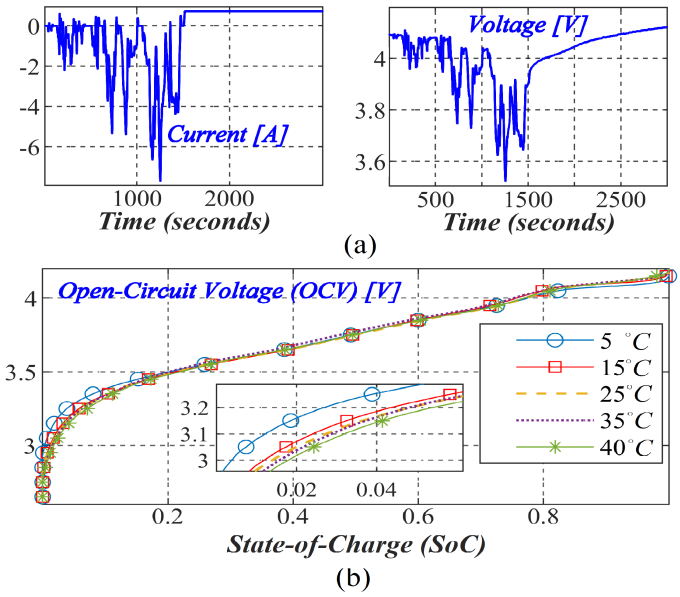

Fig. 2. (a) Current and voltage waveforms during the WLTP test cycle at 25° (b) OCV-SoC relationships for different test temperatures

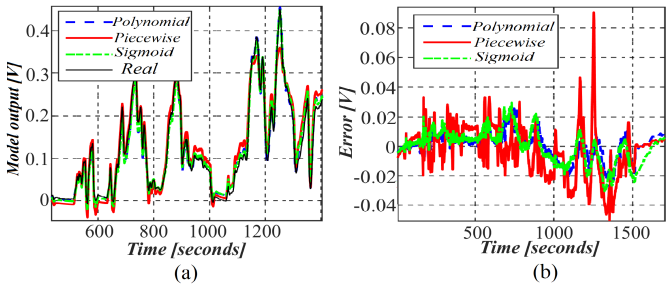

Fig. 3. (a) Outputs of different Wiener configurations fitted to the test data (b) Relevant error signals

A. Experimental Phase

NMC-based Li-ion cells with rated voltage of 3.6 V and rated capacity of 3.4 Ah were tested. The Li-ion cells were tested in a temperature-controlled environment using thermal chambers. The cells were discharged using the battery test system Digatron MCT and considering the World Harmonized Light-Duty Vehicle Test Procedure (WLTP) at different temperatures (15, 25, and 35°C). After the WLTP discharging cycle, the cells were charged to about 90% SoC with 0.68 A (0.2C), which was then followed by an idle period before iterating the tests. The cutoff voltages in charging and discharging processes were set to 4.2 V and 2.65 V, respectively. The monitoring software BTS-600 was used to record the battery data with a sampling time of 1 second. The recorded voltage and current waveforms, as well as the OCV-SoC curves at different test temperatures are shown in Fig. 2. Since the hysteresis effect of the NMC-based Li-ion batteries is negligible [26], the OCV-SoC curve is obtained by averaging the curves recorded during charging and discharging [26].

TABLE I
MEAN SQUARED ERROR OBTAINED IN SYSTEM IDENTIFICATION TESTS

Function	Model degree 1	2	3
Polynomial	3.664×10^{-4}	1.299×10^{-4}	1.263×10^{-4}
Sigmoid network	3.577×10^{-4}	1.478×10^{-4}	1.289×10^{-4}
Piecewise linear	4.153×10^{-4}	2.187×10^{-4}	1.823×10^{-4}
Second-order ECM			4.883×10^{-4}

B. System Identification Tests for Battery Modeling

MATLAB's *System Identification* toolbox is used for selection of $f(\cdot)$ as well as modeling of the OCV-SoC functions. Different functions including the Sigmoid network, polynomial functions with different orders, and Piecewise linear function are considered and tested to obtain the structure that leads to the maximum modeling accuracy. The output of the Wiener configuration shown in Fig. 1 is obtained by subtracting the battery terminal voltage from the recorded OCV data. The Levenberg-Marquardt algorithm is used to fit battery data $i_{battery}$ and v_f to the test models. Typical results are shown in Fig. 3 and Table I. The results reveal that among different functions considered in the output of the Wiener structure, the polynomial function achieves the best performance with Mean Squared Error (MSE) of about 1.3×10^{-4}, which is promising compared to the second-order ECM with MSE of 4.883×10^{-4}. The MSE is calculated using the following formula:

$$MSE = \frac{1}{N}\sum_{j=1}^{N}(v_f(j) - \hat{v}_f(j))^2 \tag{3}$$

where N is the number of sample points, $v_f(j)$ denotes the real output of the Wiener configuration at sample j, and $\hat{v}_f(j)$ denotes the estimated output of the Wiener configuration. The results reflect that increasing the model degree can provide better fitting results. However, increasing the model degree will undesirably increase the computational burden, as well. While increasing the model degree from 1 to 2 has yielded approximately twice better fitting performances in all cases, it is observable that increasing the model degree from 2 to 3 leads to a negligible performance improvement. Thus, to avoid inordinate computational complexity, the polynomial model with degree 2 is chosen for the Wiener structure. It should be noted that the SoC and parameter estimation frameworks developed in this paper are applicable to different formats of $f(\cdot)$ and thus for different batteries. Using a similar approach, a polynomial function with degree 9 is also chosen to represent the open-circuit characteristic curves (OCV-SoC functions).

C. Real-Time Estimation of Model Parameters

In practice, the model parameters might change due to the variations of the environmental or operating conditions [2]. To account for these changes, the model parameters should be

updated in real-time. Considering $f(\cdot)$ to be a second-order polynomial, one can write:

$$v_f(k) = \gamma_1 x(k) + \gamma_2 x^2(k) \tag{4}$$

Let $\gamma_1 = 1$ without loss of generality (the effect of γ_1 can be easily reflected in the coefficients of the z-polynomial $B(z^{-1})$). Combining (1) and (4) yields:

$$v_f(k) = \frac{B(z^{-1})}{A(z^{-1})} i_{battery}(k) + \gamma_2 x^2(k) \tag{5}$$

Multiplying (5) by $A(z^{-1})$ one can write:

$$A(z^{-1})v_f(k) = B(z^{-1})i_{battery}(k) + \gamma_2 A(z^{-1})x^2(k) \tag{6}$$

Adding $v_f(k)$ to the left and right sides of (6) and rearranging:

$$v_f(k) = (1 - A(z^{-1}))v_f(k) + B(z^{-1})i_{battery}(k) + \gamma_2 A(z^{-1})x^2(k) \tag{7}$$

Based on subsection II.B, the linear part of the Wiener configuration is represented by the second-order ECM, which corresponds to second-order z-polynomials $A(z^{-1})$ and $B(z^{-1})$ with $n = m = 2$. Thus, (7) can be rewritten as follows:

$$v_f(k) = -a_1 v_f(k-1) - a_2 v_f(k-2) + b_0 i_{battery}(k) + b_1 i_{battery}(k-1) + b_2 i_{battery}(k-2) + \gamma_2 x^2(k) + \gamma_2 a_1 x^2(k-1) + \gamma_2 a_2 x^2(k-2) \tag{8}$$

The regression equation can thus be written as follows:

$$v_f(k) = r^T(k)\hat{\theta}(k) + \epsilon(k) \tag{9}$$

where ϵ is the parameter estimation error. Likewise, r and $\hat{\theta}$ are, respectively, the regressor (information vector) and the estimation of the unknown parameters' vector as follows:

$$r(k) = [-v_f(k-1) \;\; -v_f(k-2) \;\; i_{battery}(k) \;\; i_{battery}(k-1) \;\; i_{battery}(k-2) \;\; x^2(k) \;\; x^2(k-1) \;\; x^2(k-2)]^T \tag{10}$$

$$\hat{\theta} = [\hat{\theta}_1 \;\; \hat{\theta}_2 \;\; \hat{\theta}_3 \;\; \hat{\theta}_4 \;\; \hat{\theta}_5 \;\; \hat{\theta}_6 \;\; \hat{\theta}_7 \;\; \hat{\theta}_8]^T = [a_1 \;\; a_2 \;\; b_0 \;\; b_1 \;\; b_2 \;\; \alpha_1 \;\; \alpha_2 \;\; \alpha_3]^T \tag{11}$$

where $\alpha_1 = \gamma_2$, $\alpha_2 = \gamma_2 a_1$, and $\alpha_3 = \gamma_2 a_2$. The objective is to find the estimation of the unknown parameters' vector $\hat{\theta}$. To realize this objective, the EKIRLS algorithm is used to minimize the following Cost Function (CF):

$$CF = \frac{1}{N}\sum_{k=1}^{N}(v_f(k) - r^T(k)\hat{\theta}(k))^2 \tag{12}$$

with N being the length of the data window. To minimize (12) with respect to $\hat{\theta}$, the parameters vector and the covariance matrix of the estimation error P must be updated in a recursive manner through the following equations:

$$K(k) = \frac{P(k-1)r(k)}{1 + r^T(k)P(k-1)r(k)} \tag{13}$$

$$\hat{\theta}(k) = \hat{\theta}(k-1) + K(k)[v_f(k) - r^T(k)\hat{\theta}(k-1)] \tag{14}$$

$$P(k) = (I - K(k)r^T(k))P(k-1) \tag{15}$$

where K is the gain of the filter. Equations (13)-(15) cannot be directly used to obtain $\hat{\theta}$ because in the information vector (10), the intermediate signal $x(k)$ is not available. The EKIRLS algorithm resolves this problem through an iterative approach, which helps estimating the intermediate signal and replacing the last estimation of the information vector into (13)-(15). The estimation of (10) can be written as follows:

$$\hat{r}(k) = [-v_f(k-1) \;\; -v_f(k-2) \;\; i_{battery}(k) \;\; i_{battery}(k-1) \;\; i_{battery}(k-2) \;\; \hat{x}^2(k) \;\; \hat{x}^2(k-1) \;\; \hat{x}^2(k-2)]^T \tag{16}$$

Based on (1), the estimation of the intermediate signal can be updated using the following equation:

$$\hat{x}(k) = (1 - A(z^{-1}))\hat{x}(k-1) + B(z^{-1})i_{battery}(k) \tag{17}$$

With each incoming sample point, the EKIRLS inner iterative algorithm is active and estimates the intermediate signal x, by which the regressor equation (16) will also be updated in each iteration. According to this procedure, the parameters vector $\hat{\theta}$ can be estimated using the same set of equations (13)-(15) except that in these equations $r(k)$ must be substituted by $\hat{r}(k)$. The EKIRLS algorithm should be initialized at the first iteration, which is fulfilled as follows:

$$P(0) = 10 \times \boldsymbol{I}^{8\times 8} \;\; , \;\; \hat{\theta}(0) = \mathbf{0}^{8\times 1} \;\; , \;\; \hat{r}(0) = \mathbf{0}^{8\times 1}$$

where $\boldsymbol{I}$ and $\mathbf{0}$ are the identity and zero vectors, respectively. In the literature, sampling times between 1 to 10 seconds have been recommended for the parameter estimation. In this paper, the sampling time for all algorithms is set to 1 second. In practice, this value can be adjusted depending on the available processing resources and the requirements related to the performance boundaries, e.g. how fast the current, temperature, and SoC change.

III. SoC Estimation Based on the Proposed Model and Parameter Estimator

The state-space modeling, observability analysis, and EKF formulation are discussed in the following subsections.

A. State-Space Representation of the Wiener Model

The SoC of the battery is considered as the first state variable, i.e. $q_1 = SoC(k-1)$. Thus, the first state equation can be written as follows:

$$SoC(k) = SoC(k-1) - \frac{T_s \eta}{Q \times 3600} i_{battery}(k) \tag{18}$$

where T_s is the sampling time, Q is the capacity, and η is the Coulombic efficiency. The Coulombic efficiency is approximately equal to 1. Expanding (17) and considering the intermediate signal x as a state variable, one can write:

$$x(k) = -a_1 x(k-2) - a_2 x(k-3) + b_0 i_{battery}(k) + b_1 i_{battery}(k-1) + b_2 i_{battery}(k-2) \tag{19}$$

Based on (18) and (19) and defining $q_2 = x(k-1)$, $q_3 = x(k-2)$, and $q_4 = x(k-3)$ as new state variables and $u_1 = i_{battery}(k)$, $u_2 = i_{battery}(k-1)$, and $u_3 = i_{battery}(k-2)$

as the inputs of the system, the state space equations of the system can be obtained as follows:

$$\begin{bmatrix} q_1(k+1) \\ q_2(k+1) \\ q_3(k+1) \\ q_4(k+1) \end{bmatrix} = \begin{bmatrix} 1 & 0 & 0 & 0 \\ 0 & 0 & -a_1 & -a_2 \\ 0 & 1 & 0 & 0 \\ 0 & 0 & 1 & 0 \end{bmatrix} \times \begin{bmatrix} q_1(k) \\ q_2(k) \\ q_3(k) \\ q_4(k) \end{bmatrix} + \begin{bmatrix} \frac{T_s \eta}{Q \times 3600} & 0 & 0 \\ b_0 & b_1 & b_2 \\ 0 & 0 & 0 \\ 0 & 0 & 0 \end{bmatrix} \times \begin{bmatrix} u_1(k) \\ u_2(k) \\ u_3(k) \end{bmatrix} \quad (20)$$

The terminal voltage of the battery $v_{battery}$ is considered as the system output y as follows:

$$y = v_{battery}(k) = V_{OCV}(k-1) + x(k-1) + \gamma_2 x^2(k-1) = V_{OCV}(k-1) + q_2(k) + \gamma_2 q_2^2(k) \quad (21)$$

To ensure the model observability, the system output is considered as the fifth state variable, i.e. $q_5 = v_{battery}$. The fifth state equation can thus be obtained as follows:

$$q_5(k+1) = V_{OCV}(k) + q_2(k+1) + \gamma_2 q_2^2(k+1) \quad (22)$$

where $q_2(k+1)$ can simply be substituted from (20) and $V_{OCV}(k)$ can be substituted based on the OCV relationship obtained in subsection II.B.

B. Analysis of the Model Observability

The observability of nonlinear systems can be checked based on the rank of the observation space containing all repeated Lie derivatives. However, this will necessitate using complicated algebra to obtain the observability space for the proposed nonlinear Wiener model. An alternative approach is thus used to confirm the observability [27]. In this method, the dynamic interrelationship between the state variables will be graphically exploited using the so-called inference diagram. The inference diagram is composed of a series of nodes representing the system states, a series of links depicting the interdependence between the states (we draw a straight link $q_i \rightarrow q_j$ if q_j exists in the differential equation of q_i), the so-called Strongly Connected Components (SCCs), and root SCCs (RSCCs) [27]. The existence of a link in the inference diagram reflects whether the information of one state variable can be collected by monitoring another state variable over the time. The SCCs are the largest possible subgraphs in which each node is connected to all other nodes in that subgraph. Likewise, RSCCs are SCCs without incoming edges.

Definition 1 [27]: The necessary and sufficient condition for the system observability is that at least one node from each RSCC is a measurable quantity.

The inference diagram of the system (20)-(22) is shown in Fig. 4. As seen, the diagram contains only one RSCC, which is related to the fifth state variable. Since this state variable is measurable (it is equal to the battery terminal voltage), based on *Definition 1*, the system is observable.

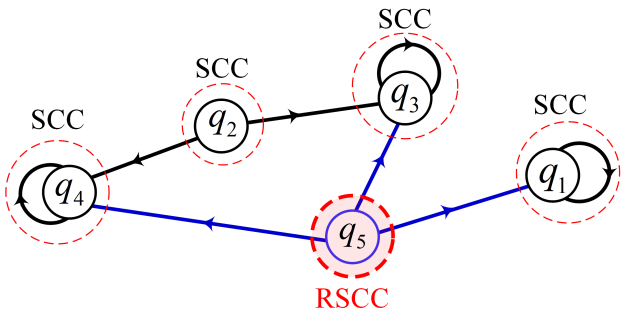

Fig. 4. Inference diagram of the battery state-space model (20)-(22)

C. Implementation of the EKF for SoC estimation

The nonlinear state-space representation of the Wiener model can be written in the following form:

$$\begin{aligned} q_k &= g_{k-1}(q_{k-1}, u_{k-1}, \omega_{k-1}) \\ y_k &= h_k(q_k, u_k, \upsilon_k) \\ \omega_k &\sim (0, Q_k) \\ \upsilon_k &\sim (0, R_k) \end{aligned} \quad (23)$$

where ω and υ are the process and measurement noises, respectively. Likewise, the third and fourth equations in (23) show that the system and measurement noises have zero mean with covariance matrices Q and R, respectively. The covariance matrices Q and R determine the levels of modeling uncertainties and measurement errors/noises, respectively. The value of R is chosen based on the accuracy level of the measurements. To determine Q, a specified range of values was considered for each diagonal entry of Q and the simulations were repeated considering different combinations of the assigned values. Accordingly, a parameters set that provided the least SoC estimation RMSE is used for the simulations [28], [29]. The values of R and Q are accordingly set as:

$$R = 0.01 \quad , \quad Q = diag(0.01, 0.01, 0.005, 0.005, 0.05)$$

In the first step, the EKF algorithm should be initialized, which is fulfilled as follows:

$$\hat{q}^+(0) = E(q(0)) = \mathbf{0^{5\times 1}}$$

$$\Phi^+(0) = E[(q(0) - \hat{q}^+(0))(q(0) - \hat{q}^+(0))^T] = 10 \times \boldsymbol{I^{5\times 5}}$$

where $\hat{q}^+$ denotes the *posteriori* estimate of the state vector, Φ^+ is the *posteriori* estimate of the covariance matrix of the estimation error, and $E[\cdot]$ is the expected value operator. Likewise, $\mathbf{0}$ and $\boldsymbol{I}$ are zero and identity matrices, respectively. The EKF algorithm includes two estimation steps. In the first step, the so-called time-update phase, a *priori* estimate of the states $\hat{x}^-$ and covariance matrix of the estimation error Φ^- are obtained as follows:

$$\Phi^-(k) = F(k-1)\Phi^+(k-1)F^T(k-1) + L(k-1)Q(k-1)L^T(k-1) \quad (24)$$

$$\hat{x}^-(k) = g_{k-1}(\hat{x}^+(k-1), u(k-1), 0) \quad (25)$$

where F and L are the partial derivative matrices. Based on the state-space representation of the battery and considering that the process and measurement noises are included in the model in an additive form, these matrices are obtained as follows:

$$F(k-1) = \frac{\partial g_{k-1}}{\partial q}|_{\hat{q}^+(k-1)} = \begin{bmatrix} 1 & 0 & 0 & 0 & 0 \\ 0 & 0 & -a_1 & -a_2 & 0 \\ 0 & 1 & 0 & 0 & 0 \\ 0 & 0 & 1 & 0 & 0 \\ \beta_1 & 0 & \beta_2 & \beta_3 & 0 \end{bmatrix} \tag{26}$$

$$L(k-1) = \frac{\partial g_{k-1}}{\partial \omega}|_{\hat{q}^+(k-1)} = \boldsymbol{I^{5\times 5}} \tag{27}$$

where β_1, β_2, and β_3 are provided in the Appendix. In the second estimation step, the so-called measurement-update phase, *posteriori* estimates of the states and the covariance matrix of the estimation error can be obtained using the following equations:

$$G = \Phi^-(k)H^T(k)(H(k)\Phi^-(k)H^T(k) + M(k)RM^T(k))^{-1} \tag{28}$$

$$\hat{q}^+(k) = \hat{q}^-(k) + G[y(k) - h_k(\hat{q}^-(k), u(k), 0)] \tag{29}$$

$$\Phi^+(k) = (I - G(k)H(k))\Phi^-(k) \tag{30}$$

where H and M are partial derivative matrices obtained as:

$$H(k) = \frac{\partial h_k}{\partial q}|_{\hat{q}^-(k)} = \begin{bmatrix} \beta_4 & 1 + 2\gamma_2 q_2(k) & 0 & 0 & 0 \end{bmatrix} \tag{31}$$

$$M = 1 \tag{32}$$

where $\beta_4 = \beta_1$ is given in the Appendix.

IV. Results and Discussion

The developed EKIRLS parameter estimation algorithm and the EKF-based SoC estimation method are implemented in MATLAB/Simulink® environment. The experimental data recorded through different validation tests based on WLTP and UDDS cycles are used to validate the proposed algorithms. The initial values of all parameters are set to zero. To provide an effective benchmark, reference performance tests (RPTs) based on applying charge and discharge current pulses were carried out and the reference values of the model parameters at different SoC and temperature conditions are accordingly obtained through offline optimizations using MathWork's Simulink® Design Optimization toolbox. Two discharge pulses and one charge pulse were considered for each SoC level and the tests were carried out at different SoC conditions including 0.1, 0.3, 0.5, 0.7, 0.9. The tests were repeated at two different test temperatures, i.e. 25°C and 35°C. The duration of the charge/discharge pulses was set to 18 seconds in the experiments and the relaxation time between the pulses was 30 minutes. The reference parameters for the model were accordingly obtained using the voltage responses to the current pulses and the Simulink® Design Optimization toolbox. To this end, the block diagram of the model was created in the Simulink® environment. The following procedure was then followed: 1- automatically generate values for different model parameters, 2- run the model to see how well voltage predictions agree with the measured data, 3-update the parameter estimates, 4- iterate until it converges on the final solution [30].

The parameter estimation results at 25°C and 35°C are shown in Fig. 5. The results show that the filter performance is stable and the estimations accurately match with the reference values of the parameters. The averaged Root MSE (RMSE) for estimation of all parameters is obtained 4.83×10^{-3} and 5.63×10^{-3} at 25°C and 35°C, respectively. In Figs. 6(a) and (b), the real and predicted values of $v_{battery}$ and the relevant error ($v_{battery} - \hat{v}_{battery}$) at 25°C are shown. It can be seen that the battery terminal voltage is precisely predicted (RMSE about 8.2 mV). The error at the start of the simulation is caused by the mismatch between the selected initial value and the real output. This confirms that the proposed method can converge to the true output irrespective of the wrong initial settings. Figs. 6(c)-(f) show the reference and estimated values of the SoC at 25°C considering different initial conditions. The real initial SoC of the cells in the experiments was set to 0.87. It is observed that in all scenarios the SoC is successfully estimated and the SoC estimation error is favorably low, i.e. RMSE about 4.9×10^{-3} and 7.3×10^{-3} at 25°C and 35°C, respectively. The transient performance is shown in Figs. 6(d)-(e), which confirm the correct convergence of the SoC to its true value. To check the long-term robustness of the filter, the test is repeated over 5 consecutive WLTP cycles. Fig. 6(f) clearly shows that the filter performance is quite stable for simulation time interval above 9 hours.

To assess the robustness of the proposed method against the measurement noises, random noise with Signal-to-Noise Ratio (SNR) of 30 dB is added to the measurements and the tests are reiterated at 25°C and considering the same simulation settings. The simulation results are displayed in Fig. 7. As seen in Fig. 7(a), the estimated voltage of the battery converges to the real terminal voltage irrespective of the wrong initial settings and noisy measurements. Although the effect of the 30dB noise on the measurements is clearly observable in Fig. 7(b) leading to high-frequency error, the proposed method still achieves favorably low prediction error with RMSE of about 0.014 V. Likewise, Figs. 7(c) and (d) show that the SoC estimation is robust against the measurement noise effects. In this scenario, the RMSE for SoC estimation is obtained 0.62.

To further validate the proposed method, it is tested on a new battery dataset consisting of repeating charging/discharging cycles. The cycles are based on the Urban Dynamometer Driving Schedule (UDDS) with rest periods in-between. The newly considered dataset drives the fully charged 5-Ah battery cells to zero SoC conditions and thus, the proposed method can be examined over the whole SoC range. Detailed information about the utilized dataset is provided in [30]. The simulation results of the proposed method at 25°C are shown in Fig. 8. Figs. 8(a) and (b) display the experimental voltage and current of the battery cells considering 19 repetitions of the UDDS cycle (with rests in between). Fig. 8(c) shows a zoomed view of the real and predicted battery voltage and the relevant modeling error is displaced in Fig. 8(d). It is seen that the terminal voltage is precisely estimated with the proposed method. The RMSE for terminal voltage prediction is obtained about 9.4 mV. Likewise, from Figs. 8(e) and (f), it

This article has been accepted for publication in a future issue of this journal, but has not been fully edited. Content may change prior to final publication. Citation information: DOI 10.1109/TIE.2021.3071679, IEEE Transactions on Industrial Electronics

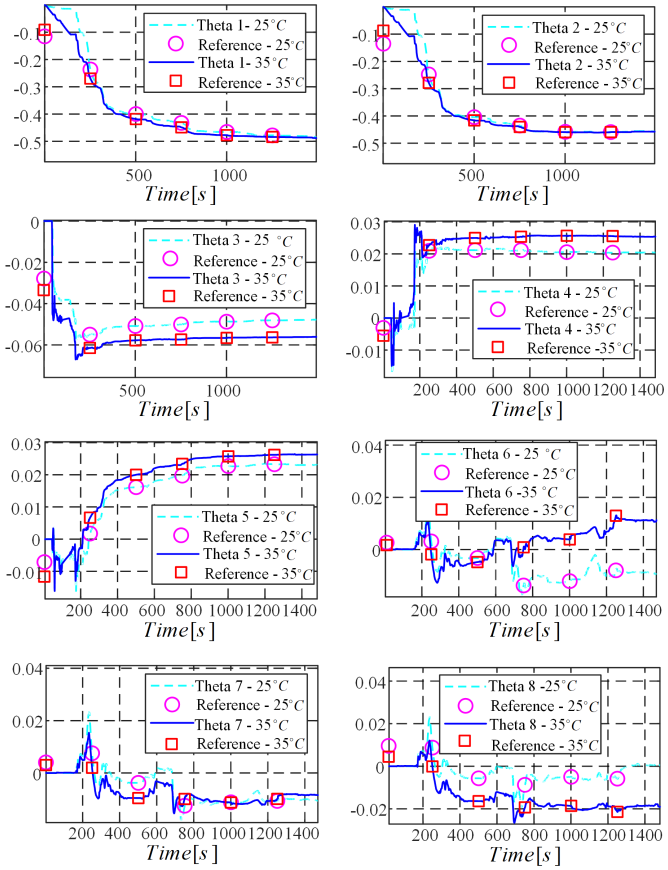

Fig. 5. Reference values and estimations of the model parameters using the proposed EKIRLS algorithm at 25℃ and 35℃

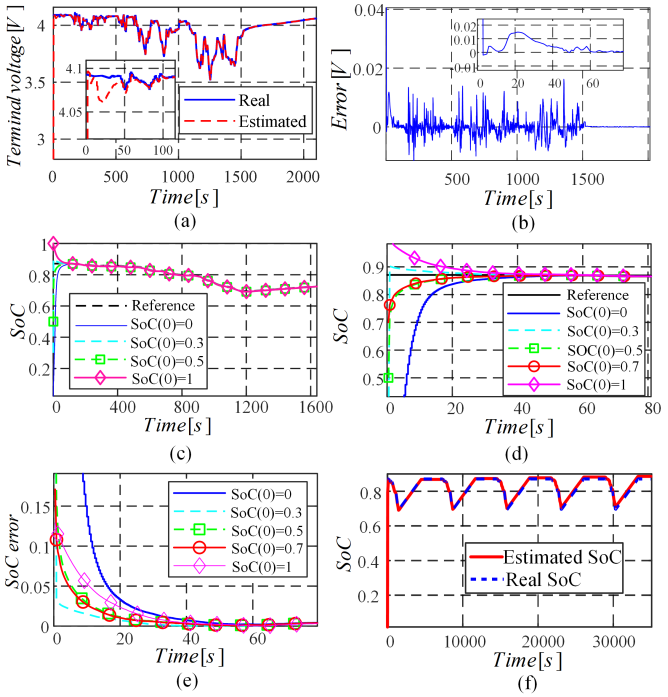

Fig. 6. (a) Real and predicted values of the battery terminal voltage at 25℃ (b) Terminal voltage error ($v_{battery} - \hat{v}_{battery}$) (c) Reference SoC and estimated SoC with different initial settings at 25℃ (d) Zoomed view of figure (c) showing convergence behavior (e) SoC error (f) Reference SoC and its estimation over several consecutive WLTP cycles

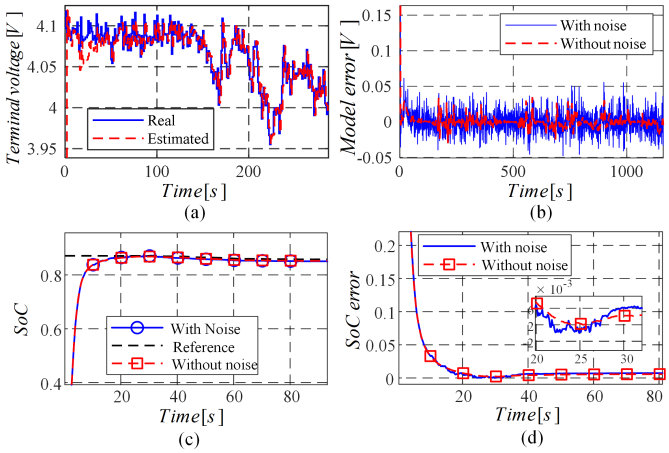

Fig. 7. (a) Real and predicted values of the battery terminal voltage when white noise with SNR=30dB is added to the battery voltage measurements (b) Model error (c) Reference and estimated values of the SoC with and without considering the noise (d) SoC estimation error with and without considering noise

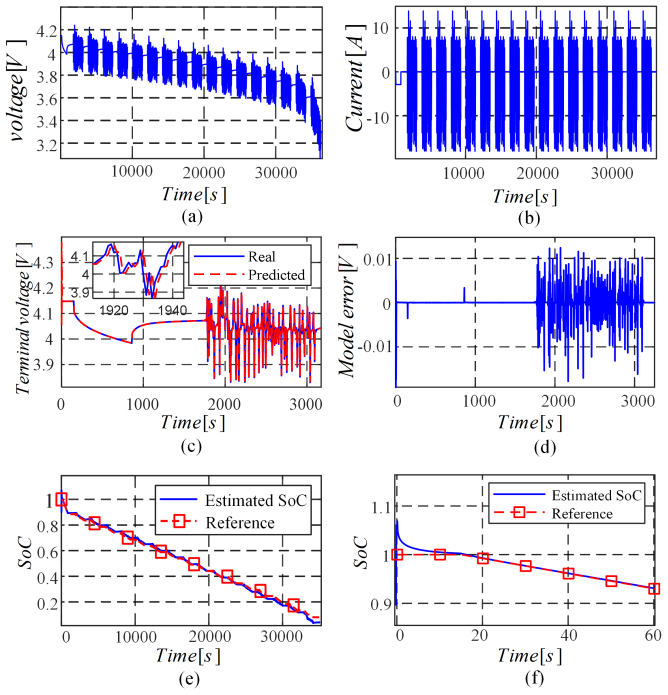

Fig. 8. (a) Experimental battery voltage over several repetitions of the UDDS test cycle with rests in-between (b) Battery current (c) Reference and predicted waveforms of the terminal voltage (d) Model error (e) Reference and estimated values of the SoC (f) Zoomed view of SoC

can be observed that the SoC estimation is precise and stable during the whole simulation time. However, under very low SoC conditions, i.e. SoC lower than 0.2, a negligible mismatch between the reference and estimated values is observable, which is caused by the polarization characteristics at the low SoC region. However, even in very low SoC conditions, the maximum SoC estimation error is lower than 0.02 and the RMSE for SoC estimation is obtained 5.4×10^{-3}, which is still very promising. Likewise, the RMSE for SoC estimation at 5°C is obtained about 6.6×10^{-3}.

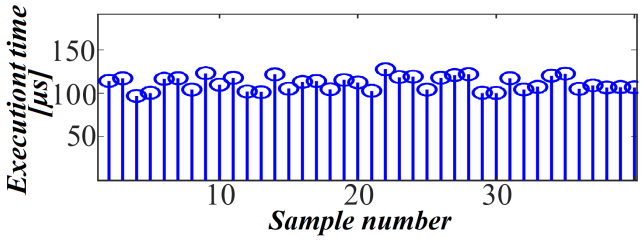

Fig. 9. Execution time of the proposed approach obtained through PiL tests based on dSPACE1104 platform

To demonstrate the feasibility of embedded implementation, PiL tests are conducted using the dSPACE1104 development platform. To this end, the MATLAB's Code Generation Option is used to generate the C code of the parameter and SoC estimation algorithm, which are totally implemented in MATLAB/Simulink® environment using a sampling time of $T_s = 1seconds$. The C code (description file) is then imported to ControlDesk software for calculating the execution time of the algorithm. The execution time of the code is calculated based on the dSPACE Real-Time Interface (RTI) through *atomic subsystems*. The results are shown in Fig. 9. As seen, the execution time changes from one sample to another, which is due to the random performance of the CPU cache. The average execution time is calculated about $110\mu seconds$. This means that considering a sampling time of $T_s = 0.1second$ and a 250 MHz processor, the proposed method (consisting of the Wiener model, EKIRLS algorithm, and EKF) is applicable for SoC estimation of a pack consisting of about 900 $(T_s/(110 \times 10^{-6}))$ battery cells. As an industrial example, TMS570LS0432 is a high-performance automotive-grade microcontroller from Texas Instruments offering a clock frequency up to 80 MHz. This processor will be sufficient to fulfill the SoC estimation (at cell-level) for a battery pack consisting of about 288 cells. However, this number can be increased by adopting higher sampling times.

V. Comparison with Other Methods

To show the advantages of the proposed method, a comparison between the proposed method and two other similar techniques presented in [22], [23], and [30] is fulfilled and the obtained results are summarized in Table II. The method proposed in [22] is based on the auto-regressive exogenous model (ARXM) and the SoC estimation has been fulfilled using the sequential Monte Carlo filter (SMCF). Likewise, in [23] and [30], the modeling and SoC estimation are fulfilled based on the second-order ECM and EKF algorithm, respectively. The comparative study is fulfilled on a common experimental dataset related to 5-Ah battery cells at two different test temperatures, i.e. 5°C and 25°C [30]. The execution times of the algorithms are computed using the dSPACE1104 platform and considering sampling time of $T_s = 1$ second. Likewise, the parameter estimation task is also considered in the real-time tests.

In Table II, AET denotes the average execution time of the algorithm. Also, the type of reported error is RMSE. Table II shows that the ARXM+SMCF approach achieves high accuracy in predicting the battery terminal voltage as well as in SoC estimation. The RMSE of the ARXM for predicting the terminal voltage is less than 21 mV and the SoC estimation error is below 2%. However, the results show that ARXM+SMCF has the highest execution time among other algorithms. On the other hand, the method based on the 2RC ECM and EKF algorithm has the lowest execution time but the errors for prediction of the terminal voltage and SoC are relatively higher. The proposed Wiener-based method achieves an excellent trade-off between the accuracy and computational efficiency among the two other approaches. The proposed method provides voltage prediction error and SoC estimation error lower than 13mV and 1%, respectively. As we could expect, the execution time is slightly larger than the 2RC+EKF, however, it is still about 1.6 times faster than the method proposed in [22]. Therefore, by incorporating the so-called Wiener structure, the proposed method can achieve results that are promising from both the accuracy and computational efficiency standpoints.

TABLE II
Comparison Between the Proposed Method and Two Similar Techniques

Reference	AET(μs)	Model error(mV)		SoC error(%)	
		5°C	25°C	5°C	25°C
[22]: ARXM+SMCF	180	20.21	15.55	1.84	1.11
[23]: 2RC ECM+EKF	90	34.86	28.31	2.47	2.31
Proposed: Wiener+EKF	110	12.51	10.72	0.93	0.51

VI. Conclusion and Future Work

In this paper, a new modeling approach based on the Wiener structure is proposed to reinforce the modeling capability of the classical ECMs. An efficient parameter estimation method based on the EKIRLS algorithm is also proposed to estimate the model parameters in real-time. The proposed method provides an excellent trade-off between the model accuracy and its real-time efficiency. The obtained results showed that the proposed method achieves excellent SoC estimation accuracy with RMSE lower than 0.95%, while its execution time is favorably low, around $110\mu seconds$ on a 250MHz processor. Thus, the combined features of being accurate and computationally efficient make the proposed approach useful for cost-driven applications. Future work can focus on the enhancement of the proposed approach to also consider the effects of battery aging. The application of advanced techniques for accurate adjustment of the covariance matrices is another interesting line of research.

Acknowledgment

This work has been a part of the transnational eVolution2Grid (V2G) project, supported by the Electric Mobility Europe (EMEurope) programme and Innovation Fund Denmark. It has been also supported by National Elites Foundation of Iran. The authors gratefully acknowledge the financial support received for carrying out this work.

APPENDIX

In (28) and (33), the parameter β_1 to β_4 are obtained as:

$$\beta_1 = 18225q_1^8 - 73888q_1^7 + 124110q_1^6 - 111900q_1^5 + 58650q_1^4 - 18096q_1^3 + 3189q_1^2 - 296.6q_1 + 12.75$$

$$\beta_2 = -a_1 - 2a_1\gamma_2(-a_1q_3 - a_2q_4 + b_0u_1 + b_1u_2 + b_2u_3)$$

$$\beta_3 = -a_2 - 2a_2\gamma_2(-a_1q_3 - a_2q_4 + b_0u_1 + b_1u_2 + b_2u_3)$$

REFERENCES

[1] J. Meng, D. Stroe, M. Ricco, G. Luo, and R. Teodorescu, "A simplified model-based state-of-charge estimation approach for lithium-ion battery with dynamic linear model," *IEEE Trans. Ind. Electron.*, vol. 66, no. 10, pp. 7717–7727, Oct. 2019.

[2] F. Naseri, E. Farjah, T. Ghanbari, Z. Kazemi, E. Schaltz, and J. Schanen, "Online parameter estimation for supercapacitor state-of-energy and state-of-health determination in vehicular applications," *IEEE Trans. Ind. Electron.*, vol. 67, no. 9, pp. 7963–7972, 2020.

[3] Y. Wang, J. Tian, Z. Sun, L. Wang, R. Xu, M. Li, and Z. Chen, "A comprehensive review of battery modeling and state estimation approaches for advanced battery management systems," *Renew. Sustain. Ener. Reviews*, vol. 131, p. 110015, 2020.

[4] X. Hu, F. Feng, K. Liu, L. Zhang, J. Xie, and B. Liu, "State estimation for advanced battery management: Key challenges and future trends," *Renewable and Sustainable Energy Reviews*, vol. 114, p. 109334, 2019.

[5] M. Corno, "Efficient control-oriented coupled electrochemical thermal modeling of li-ion cells," *IEEE Trans. Ind. Electron.*, 2020.

[6] C. Zou, X. Hu, S. Dey, and L. Zhang, "Nonlinear fractional-order estimator with guaranteed robustness and stability for lithium-ion batteries," *IEEE Trans. Ind. Electron.*, vol. 65, no. 7, pp. 5951–5961, 2018.

[7] E. Chemali, P. J. Kollmeyer, M. Preindl, R. Ahmed, and A. Emadi, "Long short-term memory networks for accurate state-of-charge estimation of li-ion batteries," *IEEE Trans. Ind. Electron.*, vol. 65, no. 8, pp. 6730–6739, 2018.

[8] G. O. Sahinoglu, M. Pajovic, Z. Sahinoglu, Y. Wang, P. V. Orlik, and T. Wada, "Battery state-of-charge estimation based on regular/recurrent gaussian process regression," *IEEE Trans. Ind. Electron.*, vol. 65, no. 5, pp. 4311–4321, 2018.

[9] C. Liu, Q. Zhu, L. Li, W. Liu, L. Wang, N. Xiong, and X. Wang, "A state of charge estimation method based on h_∞ observer for switched systems of lithium-ion nickel-manganese-cobalt batteries," *IEEE Trans. Ind. Electron.*, vol. 64, no. 10, pp. 8128–8137, 2017.

[10] S. Li, K. Li, E. Xiao, and C. Wong, "Joint soc and soh estimation for zinc-nickel single-flow batteries," *IEEE Trans. Ind. Electron.*, vol. 67, no. 10, pp. 8484–8494, 2020.

[11] R. Xiong, L. Li, Q. Yu, Q. Jin, and R. Yang, "A set membership theory based parameter and state of charge co-estimation method for all-climate batteries," *Journal of Cleaner Production*, vol. 249, p. 119380, 2020.

[12] X. Shu, G. Li, J. Shen, Z. Lei, Z. Chen, and Y. Liu, "An adaptive multi-state estimation algorithm for lithium-ion batteries incorporating temperature compensation," *Energy*, vol. 207, p. 118262, 2020.

[13] X. Shu, G. Li, J. Shen, W. Yan, Z. Chen, and Y. Liu, "An adaptive fusion estimation algorithm for state of charge of lithium-ion batteries considering wide operating temperature and degradation," *Journal of Power Sources*, vol. 462, p. 228132, 2020.

[14] Z. Wei, C. Zou, F. Leng, B. H. Soong, and K. Tseng, "Online model identification and state-of-charge estimate for lithium-ion battery with a recursive total least squares-based observer," *IEEE Trans. Ind. Electron.*, vol. 65, no. 2, pp. 1336–1346, 2018.

[15] W. Gao, Y. Zheng, M. Ouyang, J. Li, X. Lai, and X. Hu, "Micro-short-circuit diagnosis for series-connected lithium-ion battery packs using mean-difference model," *IEEE Trans. Ind. Electron.*, vol. 66, no. 3, pp. 2132–2142, 2019.

[16] Z. Wei, G. Dong, X. Zhang, J. Pou, Z. Quan, and H. He, "Noise-immune model identification and state-of-charge estimation for lithium-ion battery using bilinear parameterization," *IEEE Trans. Ind. Electron.*, vol. 68, no. 1, pp. 312–323, 2020.

[17] S. Nejad and D. T. Gladwin, "Online battery state of power prediction using prbs and extended kalman filter," *IEEE Trans. Ind. Electron.*, vol. 67, no. 5, pp. 3747–3755, 2020.

[18] M. Cai, W. Chen, and X. Tan, "Battery state-of-charge estimation based on a dual unscented kalman filter and fractional variable-order model," *Energies*, vol. 10, no. 10, p. 1577, 2017.

[19] S. Kim, H. J. Park, J. Choi, and D. Kwon, "A novel prognostics approach using shifting kernel particle filter of li-ion batteries under state changes," *IEEE Trans. Ind. Electron.*, 2020.

[20] T. Mesbahi, N. Rizoug, P. Bartholomeus, R. Sadoun, F. Khenfri, and P. Le Moigne, "Dynamic model of li-ion batteries incorporating electrothermal and ageing aspects for electric vehicle applications," *IEEE Trans. Ind. Electron.*, vol. 65, no. 2, pp. 1298–1305, 2018.

[21] K. Smith and C.-Y. Wang, "Solid-state diffusion limitations on pulse operation of a lithium ion cell for hybrid electric vehicles," *Journal of Power Sources*, vol. 161, no. 1, pp. 628 – 639, 2006.

[22] G. Dong, Z. Chen, and J. Wei, "Sequential monte carlo filter for state-of-charge estimation of lithium-ion batteries based on auto regressive exogenous model," *IEEE Trans. Ind. Electron.*, vol. 66, no. 11, pp. 8533–8544, 2019.

[23] K. Li, F. Wei, K. J. Tseng, and B. Soong, "A practical lithium-ion battery model for state of energy and voltage responses prediction incorporating temperature and ageing effects," *IEEE Trans. Ind. Electron.*, vol. 65, no. 8, pp. 6696–6708, 2018.

[24] M. Kazemi and M. M. Arefi, "A fast iterative recursive least squares algorithm for wiener model identification of highly nonlinear systems," *ISA Transactions*, vol. 67, pp. 382–388, 2017.

[25] W. Allafi, K. Uddin, C. Zhang, R. Mazuir, R. Ahsan, and J. Marcoa, "On-line scheme for parameter estimation of nonlinear lithium ion battery equivalent circuit models using the simplified refined instrumental variable method for a modified wiener continuous-time model," *Applied Energy*, vol. 204, pp. 497–508, 2017.

[26] A. Gismero, E. Schaltz, and D. Stroe, "Recursive state of charge and state of health estimation method for lithium-ion batteries based on coulomb counting and open circuit voltage," *Energies*, vol. 13, no. 7, p. 1811, 2020.

[27] Y.-Y. Liu, J.-J. Slotine, and A.-L. Barabási, "Observability of complex systems," *Proceedings of the National Academy of Sciences*, vol. 110, no. 7, pp. 2460–2465, 2013.

[28] F. Naseri, Z. Kazemi, M. M. Arefi, and E. Farjah, "Fast discrimination of transformer magnetizing current from internal faults: An extended kalman filter-based approach," *IEEE Transactions on Power Delivery*, vol. 33, no. 1, pp. 110–118, 2017.

[29] F. Naseri, Z. Kazemi, E. Farjah, and T. Ghanbari, "Fast detection and compensation of current transformer saturation using extended kalman filter," *IEEE Transactions on Power Delivery*, vol. 34, no. 3, pp. 1087–1097, 2019.

[30] G. L. Plett, *Battery management systems, Volume II: Equivalent-circuit methods*. Artech House, 2015.

Farshid Naseri received the B.Sc. degree in electrical engineering from Shiraz University of Technology, Shiraz, Iran, in 2013, and the M.Sc. and Ph.D. degrees in power electronics from Shiraz University, Shiraz, Iran, in 2015 and 2019, respectively. In 2019, he joined the Electro-Mobility and Industrial Drives research program at the Department of Energy Technology, Aalborg, Denmark as a guest researcher. Since 2020, he has been working as a postdoctoral fellow at the Department of Electrical and Computer Engineering, Shiraz University. In his postdoctoral project which is funded by the National Elites Foundation of Iran, he is working on software design for automotive-grade battery management systems to fulfill the state estimation, balancing, and protection of the lithium-ion batteries. His current research interests include electric vehicles, power electronics, hybrid energy storage systems, and design of management systems for the battery and supercapacitor energy storage systems.

Erik Schaltz received the M.Sc. and Ph.D. degrees in electrical engineering from the Department of Energy Technology, Aalborg University, Aalborg, Denmark, in 2005 and 2010, respectively. From 2009 to 2012, he was working as an Assistant Professor with the Department of Energy Technology, Aalborg University, where he is currently working as an Associate Professor. At the department, he is the Programme Leader of the research programme in e-mobility and industrial drives and the Vice Programme Leader of battery storage systems. His research interests include analysis, modeling, design, and control of power electronics, electric machines, energy storage devices including batteries and ultracapacitors, fuel cells, hybrid electric vehicles, thermoelectric generators, reliability, and inductive power transfer systems.

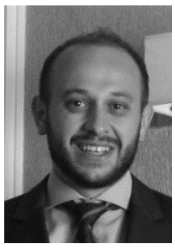

Daniel-Ioan Stroe received the Dipl.Ing. degree in automatics from the Transilvania University of Brasov, Brasov, Romania, in 2008, and the M.Sc. degree in wind power systems and the Ph.D. degree in lifetime modelling of Lithiumion batteries from Aalborg University, Aalborg, Denmark, in 2010 and 2014, respectively. He is currently an Assistant Professor with the Department of Energy Technology, Aalborg University. He was a Visiting Researcher at RWTH Aachen, Germany, in 2013. He has co-authored more than 70 journals and conference papers. His current research interests include energy storage systems for grid and e-mobility, Lithium-based batteries testing and modelling, and lifetime estimation of Lithium-ion batteries.

Alejandro Gismero received the B.Sc. and M.Sc. degree in Industrial Engineering from Polytechnic University of Madrid (ETSII-UPM), Spain, in 2017 and 2018. From 2018 to 2020, he was working as Research Assistant at the Department of Energy Technology, Aalborg University, where he is currently a PhD student. His research interests include energy storage systems for grid and e-mobility, Lithium-ion batteries testing and modelling, and design of battery management and diagnostic systems.

Ebrahim Farjah received the B.Sc. degree in electrical and electronics engineering from Shiraz University, Iran, in 1987, the M.Sc. degree in electrical power engineering from Sharif University of Technology, Tehran, Iran, in 1989, and the Ph.D. degree in electrical engineering from Grenoble Institute of Technology, Grenoble, France. He is currently a Professor in the Department of Electrical and Computer Engineering of Shiraz University. His research interests include power electronics, renewable energy, micro-grids, and power quality.